Origins of stereospecificity in DNA damage by *anti*-benzo[*a*]pyrene diol-epoxides

A molecular modelling study

Laurence H. Pearl and Stephen Neidle

Cancer Research Campaign Biomolecular Structure Unit, Institute of Cancer Research, Sutton SM2 5PX, England

Received 30 September 1986

A general computational procedure for the modelling of intercalated DNA-ligand complexes has been developed, and is used here to model intercalated complexes of the (+)-*anti* and (−)-*anti* enantiomers of benzo[*a*]pyrene diol-epoxide (BPDE) with cytosine-3′,5′-guanosine double-stranded DNA sequences (dCpG). Results are presented indicating differences between the behaviours of the two enantiomers which have implications for the understanding of the stereospecificity of DNA strand breakage by benzo[*a*]pyrene diol-epoxides.

DNA damage *Benzo*[a]*pyrene* *Intercalation* *DNA* *Molecular modelling* *Single-strand cleavage mechanism*

1. INTRODUCTION

Benzo[*a*]pyrene was identified as a potent carcinogen as early as 1933 [1]. Following this, much effort was expended in attempting to determine structure-activity relationships for compounds of this type, until it was realised that the ultimate carcinogens were more probably metabolites of the hydrocarbons [2,3], particularly dihydrodiol-epoxide derivatives where the epoxide ring is vicinal to a concavity in the edge of the hydrocarbon plane, the so-called 'bay region' [4].

Of the four possible enantiomers of benzo[*a*]pyrene 7,8-diol-9,10-epoxide, metabolic activation involves predominantly the 7*R*,8*S*-diol-9*S*,10*R*-epoxide (the (+)-*anti* form), with minor contributions from the 7*S*,8*R*,9*R*,10*S* (the (−)-*anti*) and 7*R*,8*S*,9*R*,10*S* (the (−)-*syn*) forms (fig.1). The (+)-*anti* has by far the highest mutagenicity [5], and tumorigenicity [6] of the enantiomers. Interaction of (+)-*anti*-BPDE with DNA is known to result in the formation of stable covalent adducts (primarily with guanosine

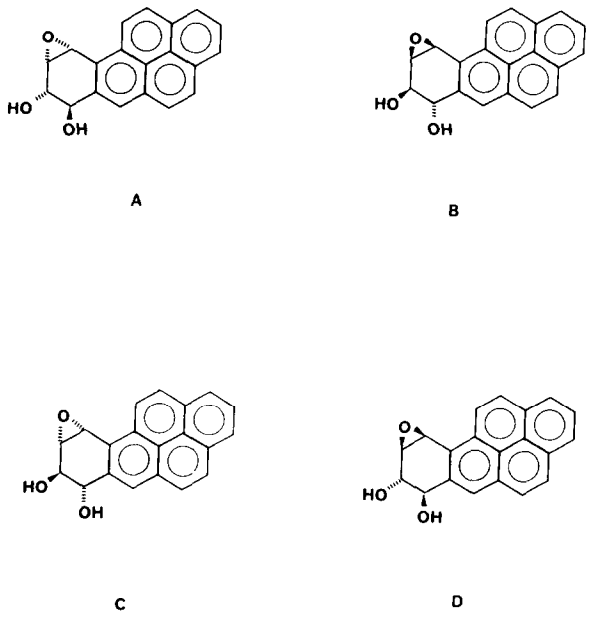

Fig.1. Stereoisomers of benzo[*a*]pyrene 7,8-diol-9,10-epoxide. (a) (+)-*anti*, (b) (−)-*anti*, (c) (+)-*syn*, (d) (−)-*syn*.

Published by Elsevier Science Publishers B.V. (Biomedical Division)
00145793/86/$3.50

residues at the exocyclic N2 position) [7,8], alkali-labile adducts resulting in depurination [9–11], and single-strand breaks at neutral pH [12,13]. Recent results [14] have shown single-strand breakage to be significantly sequence specific, primarily occurring at pyrimidine-3′,5′-guanine sites, and highly specific single-strand lesions leading to point mutations have been generated in vitro by *anti*-BPDE in the Ha-*ras* gene, leading to oncogenic activation upon transfection [15].

That the degree but not the pattern of site-specific cleavage is increased by hot alkali treatment of DNA exposed to *anti*-BPDE [14,16] suggests that the mechanism of single-strand breakage involves the formation of guanine N7-BPDE covalent adducts whose weakened glycosidic bonds lead to depurination, yielding apurinic sites which are labile to alkali cleavage [17].

Earlier molecular modelling studies [18] have investigated the general interactions possible between BPDE enantiomers and DNA in a non-covalent intercalated complex. Here, we explore the specific interactions that may lead to formation of a labile guanine N7 covalent adduct, and the limitations imposed upon the formation of such an adduct by the stereochemistry of the BPDE ligand.

2. EXPERIMENTAL

Coordinates for the intercalated double-stranded dCpG and all BPDE enantiomers derive from X-ray crystallographic studies of drug-dinucleotide intercalation complexes, and of BPDE stereoisomers [19–21].

Coordinates of the initial intercalation complexes were generated by the following procedure.

2.1. *Generation of local DNA axes*

(i) The DNA coordinates were translated so that the centroid of the atoms forming the base pairs lies at the origin of cartesian space;

(ii) The helix axis was calculated as the resultant of the normals to the least-squares planes of the two base pairs forming the intercalation site, and the coordinates of the DNA were rotated so that the helix axis lay parallel to the cartesian z axis, setting the planes of the base pairs parallel to the x-y plane;

(iii) The resultant of the major inertial axes of the two base pairs was calculated, and the DNA coordinates from the previous step were rotated around the z axis so that this resultant major axis became aligned with the cartesian x axis, thus defining the local x axis, and fixing the y axis as the mutual perpendicular of the x and z axes, such that the direction of positive increase gave a right-handed set.

2.2. *Alignment of ligand*

(i) The coordinates of the ligand were translated so that the centroid of the atoms forming the intercalating segment coincided with the centroid of the DNA atoms of the base pairs forming the intercalation site;

(ii) The least-squares plane of the atoms forming the intercalating segment of the ligand was calculated, and the coordinates transformed so that the normal to this plane lay parallel to the planes of the base pairs forming the intercalation site;

(iii) The major inertial axis of the intercalating segment of the ligand was calculated, and the coordinates rotated around the z axis so that the major axis was aligned with the x axis (fig.2).

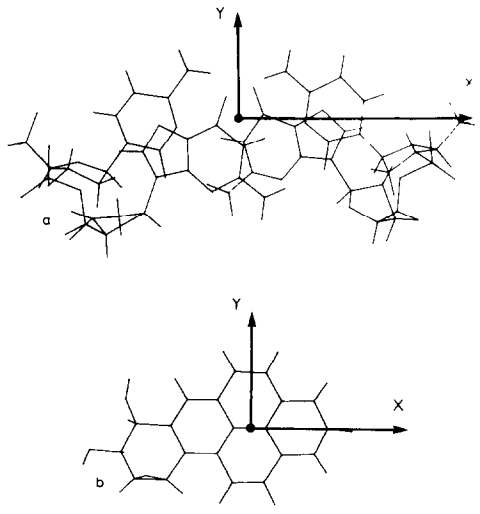

Fig.2. Initial intercalation geometry. (a) Local axes shown superimposed on DNA intercalation site, and (b) shown imposed on (+)-*anti*-BPDE. The initial intercalation geometry is achieved by alignment of the centroids (marked with a spot), in the orientation shown.

The position of the BPDE ligand relative to the DNA was thus defined with respect to this initial conformation by three parameters, u and v being respectively the components parallel to the x and y axes of the vector relating the centroid of the intercalation base pairs to the centroid of the intercalating segment of the ligand, and θ, the angle of rotation around the z axis between the major axis of the intercalation site base pairs, and the major axis of the intercalating segment of the ligand (fig.3).

Intermolecular interaction energies were calculated using a conventional molecular mechanics force field incorporating electrostatic and Lennard-Jones terms. The non-bonded interaction energy between the two atoms i and j is given by:

$$E_{ij} = \frac{q_i q_j}{rD} + \frac{A}{r^{12}} - \frac{B}{r^6}$$

where r_{ij} is the distance between the interacting pair of atoms, q_i and q_j are their point charges, and A and B are respectively the repulsive and attractive components of the Lennard-Jones potential. The dielectric constant D is linearly dependent on r_{ij}.

The values of the partial charges for the DNA are from [22], while those for the BPDE were calculated by the CNDO/2 method. The values for the Lennard-Jones parameters for all atoms are from [23]. Hydrogen atoms are treated explicitly in both electrostatic and Lennard-Jones terms.

This initial intercalation complex was used as the starting point for three procedures:

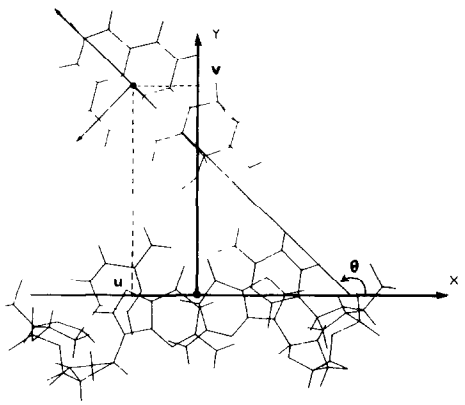

Fig.3. Definition of intercalation variables.

(1) Location of energy minima by rigid body docking with respect to u, v and θ;
(2) Scanning of the intercalation energy space as a function of u, v and θ;
(3) Monitoring the distances between guanine N7 atoms, and the reactive epoxide ring oxygen O109 of BPDE.

(1) *Location of energy minima*

The BPDE was positioned relative to the dinucleoside in the initial geometry defined above, with the parameters u and v initially zero. Rigid body energy minimisations were performed starting at eight different values of θ at 45° intervals between 0 and 360°. Interaction energies and derivatives were calculated as described above and minimisations with respect to the parameters u, v and θ were performed using a variable metric technique [24,25] and were run interactively on a VAX 11/750.

(2) *Energy scans*

The BPDE was positioned as described above, and the interaction energy of the BPDE and the DNA was calculated for values of u between -2.5 to $+2.5$ Å, v between -3.5 to $+3.5$ Å both in steps of 0.25 Å, and values of θ varying from 170 to 370° in steps of 10°.

(3) *Distance scans*

The BPDE was positioned as described above, and the distance to the N7 atom of the guanine on the same side of the pyrene plane as the epoxide ring oxygen O109 was calculated for values of u between -2.5 to $+2.5$ Å, v between -3.5 to $+3.5$ Å both in steps of 0.25 Å, and values of θ varying from 170 to 370° in steps of 10°.

3. RESULTS

3.1. *Location of energy minima*

Energy minima for the (+)-*anti* and (−)-*anti* enantiomers located by the rigid body docking procedure are given in table 1, along with the shortest guanine N7–BPDE epoxide oxygen distances possible at these minimum positions. Values of θ between 180 and 360° correspond to the diol-epoxide grouping in the major groove.

It is clear from these results that there are a range of minima of comparable energy, available

Table 1

Intercalation energy minima for (+)-*anti*-BPDE (a) and (−)-*anti*-BPDE (b)

E_{inter} (kcal)	u (Å)	v (Å)	θ (°)	D_{O-N} (Å)[a]
(a) (+)-*anti*-BPDE				
−69.7	−1.001	−0.571	315.6	3.00[b]
−68.6	−0.193	−0.584	319.3	2.46[b]
−68.2	−0.104	−0.103	322.8	2.47[b]
−65.9	0.002	0.031	202.5	5.67
−65.6	1.017	−0.782	44.4	6.86
−65.5	−0.295	0.271	105.6	6.63
−64.4	0.552	0.096	210.3	5.92
−62.1	−2.505	0.824	131.1	5.51
(b) (−)-*anti*-BPDE				
−71.5	1.393	−0.107	31.7	7.24
−66.5	−0.201	−0.657	219.3	3.85
−63.8	0.300	−0.099	328.9	5.09
−61.3	−0.178	−1.334	247.8	5.22
−61.0	1.887	1.717	12.1	5.49
−60.8	1.316	−0.240	80.8	6.35
−59.3	−1.495	0.188	83.6	6.70
−56.5	0.764	−0.139	270.6	6.34

[a] This distance is defined between N7 of guanine and O109 of BPDE

[b] These distances represent atoms within van der Waals contact

for both enantiomers. This is in marked contrast with our observations for other intercalators such as substituted acridines and anthraquinones [26] which tend to have fewer and more clearly defined minimum energy positions. The lack of any significant difference in the energy minimum values obtained for the two BPDE enantiomers would suggest that both would be capable of forming favourable intercalation complexes with a C-3′,5′-G double-stranded DNA sequence. Where they do differ most markedly however, is in the proximity of the reactive epoxide ring oxygen to the guanine N7 atom: the (−)-*anti* enantiomer cannot make a close contact at any of its minima, whereas the (+)-*anti* enantiomer has distances within van der Waals contact for its three lowest energy positions (fig.4).

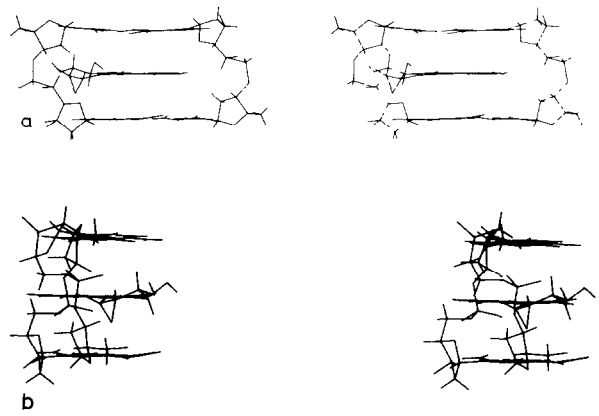

Fig.4. Structure of potentially reactive interaction of (+)-*anti*-BPDE and dCpG. Stereo pairs of a complex between (+)-*anti*-BPDE and the dCpG duplex with a favourable interaction energy and a close proximity between the epoxide of BPDE and the N7 atom of guanine. This conformation was located by rigid body minimisation (see text), and corresponds to the second minimum in table 1a. (a) View along the local y axis, and (b) view along the local x axis.

3.2. *Energy and distance scans*

Largely as a result of the multiple minima located in the rigid body docking procedure, energy and epoxide–N7 distance scans were performed for both enantiomers. Contour maps of the interaction energy and the 3.0 Å N7–epoxide distance in regions of interest for both enantiomers are shown in figs 5 and 6. The energy hypersurfaces revealed by these scans confirm the observation from the rigid body minimisation, of a broad function with no clearly delimited global minimum, for both enantiomers. The superimposed distance contours similarly confirm the availability of a large low-energy region of the hyperspace for the (+)-*anti* enantiomer, within which the guanine N7 and BPDE epoxide groups are capable of coming into close and probably reactive proximity particularly in the regions with $280° \geq \theta \leq 360°$, while the (−)-*anti* enantiomer shows only a very narrow coincidence of low energy and close contact, with the epoxide in the major groove, in the regions with $170° \geq \theta \leq 190°$.

Fig.5. Contour plots of interaction energy as a function of u, v and θ for (+)-*anti*-BPDE. u is horizontal and v is vertical. The position $(u,v) = (0,0)$ is marked with a cross. The circle superimposed on the sections is the 3.0 Å contour of the distance, as a function of u,v and θ, between the BPDE epoxide oxygen and the guanine N7 of the base pair on the same side of the $z = 0$ plane.

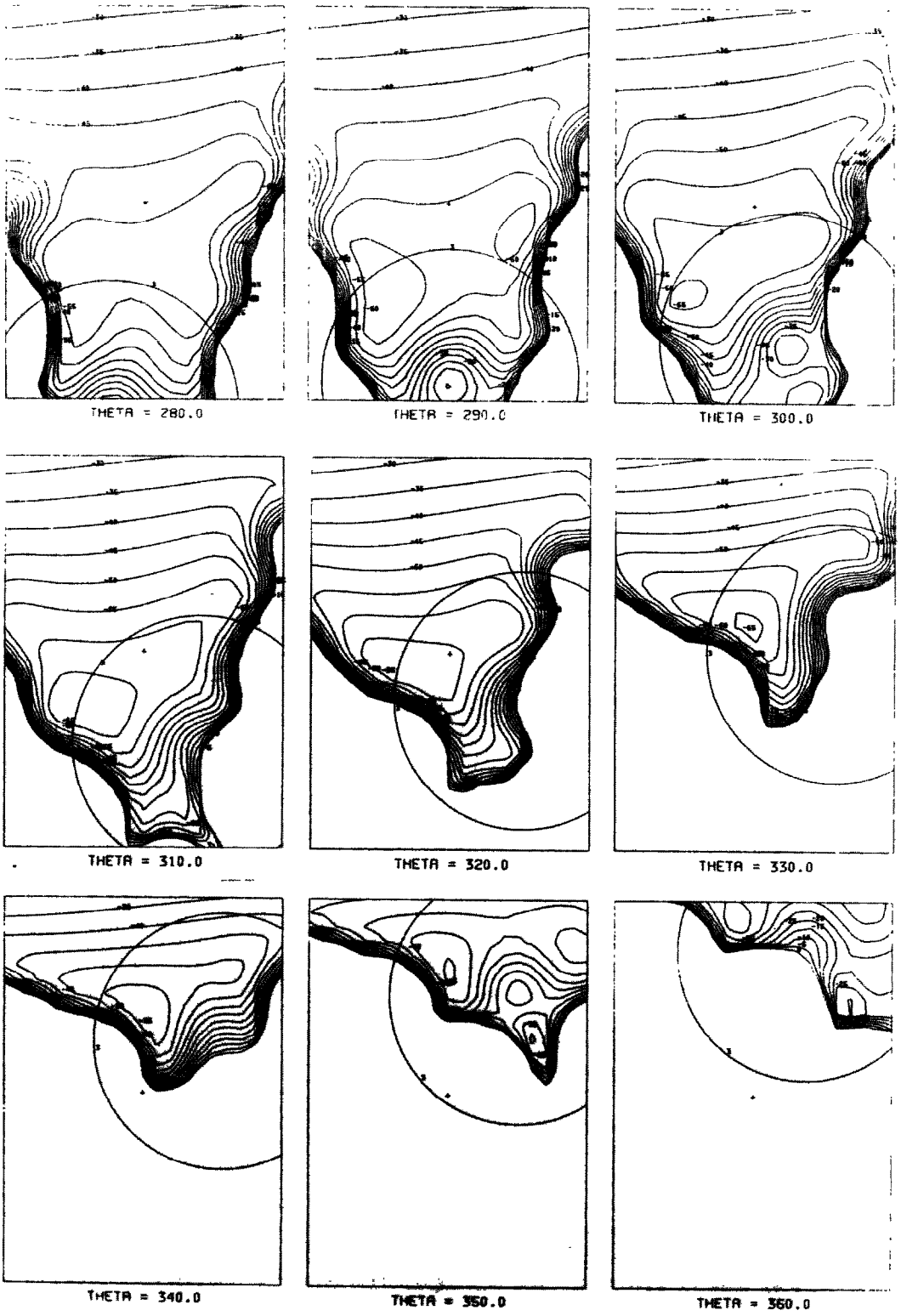
THETA = 280.0
THETA = 290.0
THETA = 300.0
THETA = 310.0
THETA = 320.0
THETA = 330.0
THETA = 340.0
THETA = 350.0
THETA = 360.0

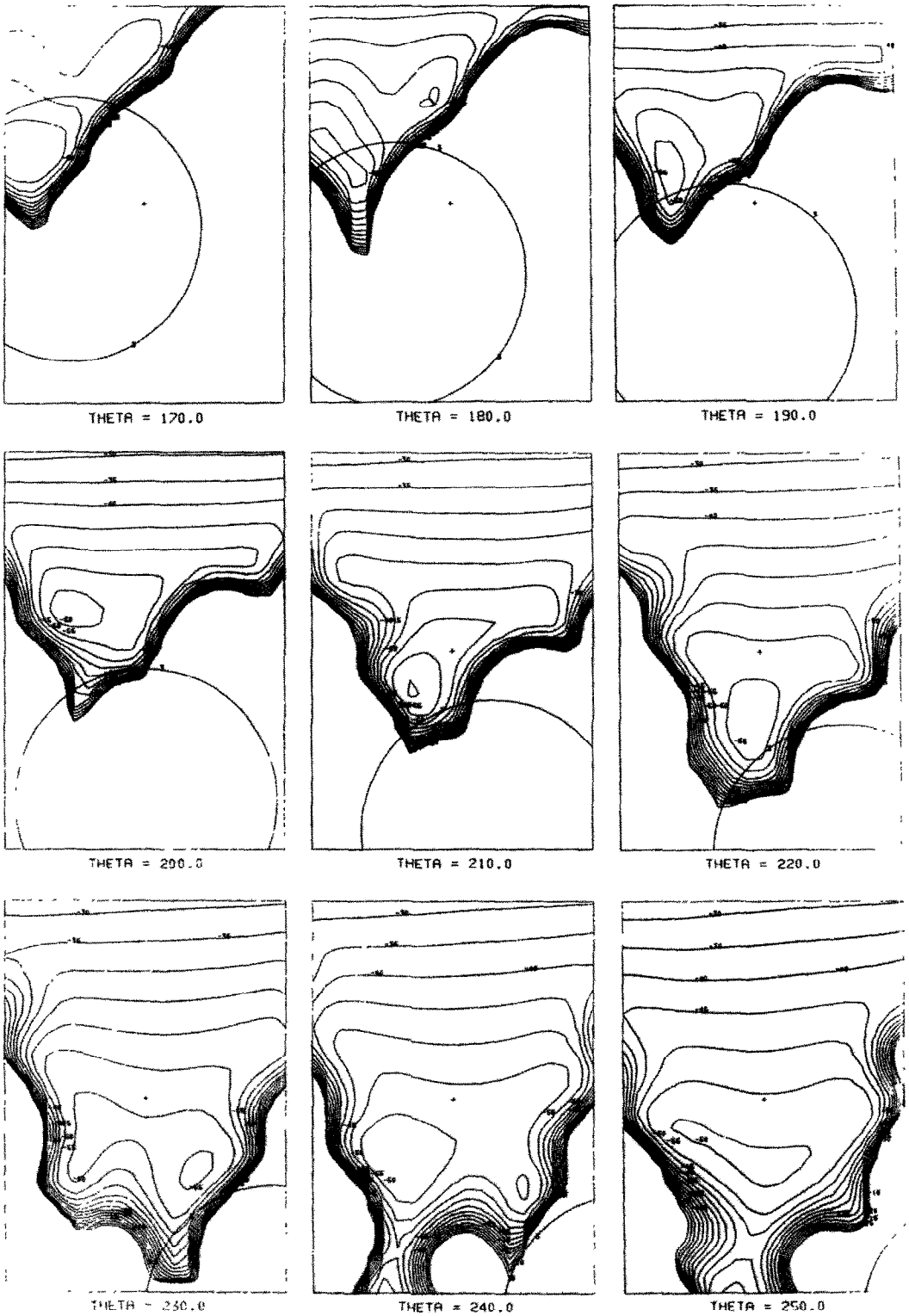

Fig.6. Contour plots of interaction energy as a function of u,v and θ for (−)-*anti*-BPDE.

4. DISCUSSION

There is much evidence that the covalent benzo[*a*]pyrene-DNA complex has the benzo[*a*]pyrene moiety situated externally in the minor groove of the helix [27–29]. Recent data are fully consistent with a classic intercalation model as the major form of initial recognition and interaction for the *anti*-diol-epoxides [30–33]. It also appears likely that the mechanism of mutagenic single-strand breakage involves depurination subsequent to the formation of an N7-attached covalent adduct. The present study shows that intercalated BPDE complexes of low energy can be modelled, which allow for a close contact (<2.5 Å) of the reactive epoxide oxygen with the guanine N7, which would be likely to proceed to formation of an N7 covalent adduct. The marked difference between the (+)-*anti* and (−)-*anti* enantiomers in their ability to achieve a potentially reactive N7-epoxide contact leads us to predict that the (−)-*anti* enantiomer would have a consequent lower activity in generating single-strand breaks, which appear to be favoured at pyrimidine-3′,5′-guanosine sites, such as the cytosine-3′,5′-guanosine sequence we have employed in this study. We are currently studying the (+)- and (−)-*syn* enantiomers of BPDE in a similar manner.

The experimentally determined preference for pyrimidine-3′,5′-guanosine sites for BPDE-induced strand breaks may be rationalised in terms of earlier findings on the sequence preferences shown by non-covalent-binding intercalative drugs and mutagens. NMR studies [34] and X-ray crystallographic analyses (e.g. [20,35]) show such a preference. These have been reinforced by energy calculations [36], which indicate that increasing the base-pair to base-pair separation from 3.4 to 6.8 Å in order to allow intercalation is energetically more favourable for a pyrimidine-3′,5′-purine sequence than for other sequences.

ACKNOWLEDGEMENTS

Drs P.L. Grover and V.V. Lobanenkov are thanked for communication of BPDE cleavage results prior to publication, and for much useful discussion.

REFERENCES

[1] Phillips, D.H. (1983) Nature 303, 468–472.
[2] Brookes, P. and Lawley, P.D. (1964) Nature 202, 781–784.
[3] Sims, P., Grover, P.L., Swaisland, A., Pal, K. and Hewer, A. (1974) Nature 252, 326–328.
[4] Lehr, R.E., Kumar, S., Levin, W., Wood, A.W., Chang, R.L., Conney, A.H., Yagi, H., Sayer, J.M. and Jerina, D.M. (1985) in: Polycyclic Hydrocarbons and Carcinogenesis (Harvey, R.G. ed.) pp.63–84, American Chemical Society, Washington.
[5] Newbold, R.F. and Brookes, P. (1976) Nature 261, 52–54.
[6] Buening, M.K., Wislocki, P.G., Levin, W., Yagi, H., Thakker, D.R., Akagi, H., Koreeda, M., Jerina, D.M. and Conney, A.H. (1978) Proc. Natl. Acad. Sci. USA 75, 5358–5361.
[7] Jeffrey, A.M., Jennette, K.W., Blobstein, S.H., Weinstein, I.B., Beland, F.A., Harvey, R.G., Kasai, H., Miura, I. and Nakanishi, K. (1976) J. Am. Chem. Soc. 98, 5714–5715.
[8] Weinstein, I.B., Jeffrey, A.M., Jennette, K.W., Blobstein, S.H., Harvey, R.G., Harris, C., Autrup, H., Kasai, H. and Nakanishi, K. (1976) Science 193, 592–595.
[9] Osborne, M.R., Harvey, R.G. and Brookes, P. (1978) Chem. Biol. Interact. 20, 123–130.
[10] King, H.W.S., Osborne, M.R. and Brookes, P. (1979) Chem. Biol. Interact. 24, 345–353.
[11] Osborne, M.R. and Merrifield, K. (1985) Chem. Biol. Interact. 53, 183–195.
[12] Gamper, H.B., Tung, A.S.-C., Straub, K., Bartholemew, J.C. and Calvin, M. (1977) Science 197, 671–674.
[13] Agarwal, K.L., Hrinyo, T.P. and Yang, N.C.-C. (1983) Biochem. Biophys. Res. Commun. 114, 14–19.
[14] Lobanenkov, V.V., Plumb, M., Goodwin, G.H. and Grover, P.L. (1986) Carcinogenesis, in press.
[15] Marshall, C.J., Vousden, K.H. and Phillips, D.H. (1984) Nature 310, 586–589.
[16] Haseltine, W.A., Lo, K.M. and D'Andrea, A.D. (1980) Science 209, 929–931.
[17] Lindahl, T. and Anderson, A. (1972) Biochemistry 11, 3618–3623.
[18] Subbiah, A., Islam, S.A. and Neidle, S. (1983) Carcinogenesis 4, 211–215.
[19] Berman, H.M., Neidle, S. and Stodola, R.K. (1978) Proc. Natl. Acad. Sci. USA 75, 828–832.
[20] Neidle, S., Subbiah, A., Cooper, C.S. and Ribeiro, O. (1980) Carcinogenesis 1, 249–254.
[21] Neidle, S. and Cutbush, S.D. (1983) Carcinogenesis 4, 415–418.

[22] Pearlstein, R.A., Dreno, P.L., Pensak, M. and Hopfinger, A.J. (1981) Biochim. Biophys. Acta 655, 432–455.
[23] Islam, S.A. and Neidle, S. (1983) Acta Crystallogr. B39, 114–119.
[24] Davidon, W.C. (1959) USAEC Document ANL5990.
[25] Fletcher, R. and Powell, M.J.D. (1963) Comput. J. 6, 163.
[26] Islam, S.A., Neidle, S., Gandecha, B.M., Partridge, M., Patterson, L.H. and Brown, J.R. (1985) J. Med. Chem. 28, 857–864.
[27] Prusik, T., Geacintov, N.E., Tobiasz, C., Ivanovic, V. and Weinstein, I.B. (1979) Photochem. Photobiol. 29, 223–232.
[28] Ridler, P.J. and Jennings, B.R. (1982) FEBS Lett. 139, 101–104.
[29] Geacintov, N.E., Gagliano, A., Ivanovic, V. and Weinstein, I.B. (1978) Biochemistry 17, 5256–5262.
[30] Geacintov, N.E., Yoshida, H., Ibanez, V. and Harvey, R.G. (1981) Biochem. Biophys. Res. Commun. 100, 1569–1577.
[31] Geacintov, N.E., Yoshida, H., Ibanez, V. and Harvey, R.G. (1982) Biochemistry 21, 1864–1869.
[32] Shahbaz, M., Geacintov, N.E. and Harvey, R.G. (1986) Biochemistry 25, 3290–3296.
[33] Geacintov, N.E. (1986) Carcinogenesis 7, 759–766.
[34] See, for example: Patel, D.J. and Canuel, L.L. (1977) Proc. Natl. Acad. Sci. USA 74, 2624–2628.
[35] Quigley, G.J., Wang, A.H.-J., Ughetto, G., Van der Marel, G., Van Boom, J.H. and Rich, A. (1980) Proc. Natl. Acad. Sci. USA 77, 7204–7208.
[36] Broyde, S. and Hingerty, B. (1979) Biopolymers 18, 2905–2910.